Environmental Science & Technology Letters

pubs.acs.org/journal/estlcu

Letter

Atmospheric OH Oxidation Chemistry of Particulate Liquid Crystal Monomers: An Emerging Persistent Organic Pollutant in Air

Qifan Liu, John Liggio,* Jeremy Wentzell, Patrick Lee, Kun Li, and Shao-Meng Li

Cite This: *Environ. Sci. Technol. Lett.* 2020, 7, 646–652

Read Online

ABSTRACT: Liquid crystal monomers (LCMs) are synthetic chemicals widely used in liquid crystal displays such as televisions and smartphones and have recently been detected in indoor dust. Despite extensive use, the atmospheric fate of LCMs is unknown. Here, the heterogeneous OH oxidation of LCMs was studied by exploring the kinetics and mechanisms of 1-ethyl-4-(4-(4-propylcyclohexyl)phenyl)benzene (EPPB) and 4′′-ethyl-2′-fluoro-4-propyl-1,1′:4′,1′′-terphenyl (EFPT) coated onto ammonium sulfate particles. The measured heterogeneous rate constants for EPPB and EFPT were $(7.05 \pm 0.46) \times 10^{-13}$ and $(4.67 \pm 0.25) \times 10^{-13}$ cm^3 molecule^{-1} s^{-1} ,respectively, equivalent to atmospheric lifetimes of up to 25 and 38 days. These lifetimes are significantly longer than previously predicted values (<1 day) for these LCMs, indicating that they are much more persistent in air than predicted, with the potential to undergo long-range transport. Furthermore, 66 transformation products from the heterogeneous photooxidation of these LCMs were identified for the first time. Given the known toxicity of the parent LCMs, their measured persistence in the atmosphere, and the demonstrated complexity of their products, the present results not only underscore the need to quantify the levels of LCMs in ambient air, but also suggest that the presence of their transformation products should not be ignored when assessing the risks of airborne LCMs.

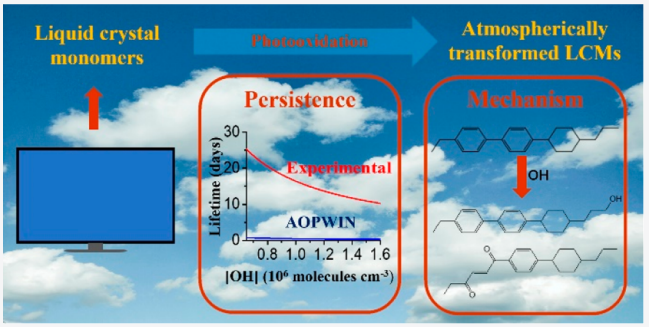

INTRODUCTION

Liquid crystal monomers (LCMs) are synthetic chemicals which generally have a diphenyl backbone structure with possible halogen substitution.[1] Due to their unique anisotropic properties,[2] LCMs are widely used in liquid crystal display (LCD) devices such as personal computers, digital televisions, and smartphones.[3] Rapid development of the LCD industry has resulted in large increases in the production of LCMs.[4] The global production of LCD panels in 2018 is 198 million m^2, which is likely to continue to increase into the future.[4,5] Given that LCMs do not covalently bind to any base materials in LCD devices, their release into the environment is expected to occur during manufacturing, utilization, and recycling of LCD devices.[3] Indeed, recent evidence indicates that LCMs are present in indoor dust.[3] The presence of LCMs in indoor dust combined with their potential to induce adverse human health effects have raised serious concerns over their environmental and health risks.[1,3,6] While data currently only exist for their presence indoors,[3] the likelihood is high that LCMs will be present in other environmental matrices such as air and water. Consequently, the risks associated with human exposure to LCMs will be linked to their persistence and reactivities in these environmental media, for which no information is currently available.

In the atmosphere, the persistence of many airborne pollutants (including LCMs) is often determined by OH-initiated oxidation reactions.[7−10] However, there are currently no published experimental reports of the atmospheric OH oxidation chemistry of LCMs. Thus, the reaction kinetics, oxidation products, degradation mechanisms, and the associated atmospheric lifetimes of airborne LCMs are unknown. Such a lack of information hampers efforts to assess their long-range transport to potentially sensitive ecosystems and the environmental impacts of their oxidation products.

In response to this lack of experimental kinetic data for LCMs, a previous study determined the atmospheric persistence of LCMs based upon AOPWIN (Atmospheric Oxidation Program for Microsoft Windows) modeled OH rate constants.[3] In that study, none of the identified LCMs from LCD devices had a predicted atmospheric lifetime of greater than 1 day, leading to the conclusion that LCMs were nonpersistent in air. However, chemical kinetic studies have clearly demonstrated that the AOPWIN model is unable to accurately predict gas-phase kinetic data for compounds

Received: June 4, 2020
Revised: July 16, 2020
Accepted: July 16, 2020
Published: July 16, 2020

https://dx.doi.org/10.1021/acs.estlett.0c00447
Environ. Sci. Technol. Lett. 2020, 7, 646–652

Table 1. Experimentally Derived and AOPWIN Predicted Parameters (Rate Constants k and Atmospheric Lifetimes τ) for two LCMs (EPPB and EFPT) and two Phosphate Flame Retardants (TDCPP and EHDP)

	k ($\times 10^{-13}$ cm^3 molecule^{-1} s^{-1})		$\tau_{\_low\ OH}$ (days)[c]		$\tau_{\_high\ OH}$ (days)[d]		
Chemicals	Particle-phase	AOPWIN	Particle-phase	AOPWIN	Particle-phase	AOPWIN	$\tau_{particle\text{-}phase}/\tau_{AOPWIN}$
EPPB	7.05 ± 0.46	242.3	25.3	0.7	10.3	0.3	34.4
EFPT	4.67 ± 0.25	127.0	38.1	1.4	15.5	0.6	27.2
TDCPP[a]	9.20 ± 0.92	180.8	19.4	1.0	7.9	0.4	19.7
EHDP[b]	11.2 ± 2.2	398.5	15.9	0.5	6.5	0.2	35.6

[a]TDCPP: tris-1,3-dichloro-2-propyl phosphate.[15] [b]EHDP: 2-ethylhexyl diphenyl phosphate.[23] [c]Low OH: OH concentration = 6.5×10^5 molecules cm^{-3}.[39] [d]High OH: OH concentration = 1.6×10^6 molecules cm^{-3}.[39]

beyond its application domain.[11−14] This issue may be further exacerbated in the case of many LCMs such as 1-ethyl-4-(4-(4-propylcyclohexyl)phenyl)benzene (EPPB) and 4′′-ethyl-2′-fluoro-4-propyl-1,1′:4′,1′′-terphenyl (EFPT), which primarily reside in the particle phase as a result of their low volatilities.[3] The atmospheric persistence of such low volatility compounds is likely to be governed by heterogeneous photooxidation (rather than gas-phase reactions), which currently cannot be accurately modeled.[15−18] The lack of information on the heterogeneous products of LCMs present a further challenge for the risk assessment of atmospherically transformed particulate LCMs. Given that the majority of LCMs are expected to be present in the particle phase, experimental investigation of the heterogeneous processing of particulate LCMs is a clear priority in order to comprehend the atmospheric fate of these compounds.

Here, the heterogeneous OH reactions of two representative LCMs (EPPB and EFPT) which have been coated onto the surface of ammonium sulfate seed particles (i.e., a proxy for pre-existing airborne particles) were studied. These two LCMs have been commonly identified in frequently used commercial LCD devices, contain functionalities similar to the majority of other LCMs (i.e., phenyl, cyclohexyl, or fluorophenyl groups), and are dominantly in the particle phase (owing to their low volatilities).[3] Using a combination of advanced mass spectrometry techniques, the heterogeneous rate constants, particulate oxidation products, and the associated oxidation mechanisms from the photooxidation of particulate LCMs are reported for the first time. These results suggest a much higher persistence for LCMs than previously assumed and highlight the importance of a comprehensive kinetic and mechanistic investigation of the atmospheric transformations of LCMs. Together, the results can potentially inform regulatory needs for these emerging chemicals.

MATERIALS AND METHODS

Oxidation Flow Reactor (OFR) Experiments. Experiments investigating the heterogeneous OH reactions with EPPB and EFPT coated onto ammonium sulfate (AS) particles were performed using an OFR (see SI).[15,16] The AS particles were generated by atomizing a 5.3 mM AS solution using a TSI atomizer (model 3706) and dried by a TSI diffusion drier (model 3062). The dry AS particles then passed through a heated Pyrex glass tube (343 K) in the presence of a LCM. This approach resulted in particles with a coating thickness of approximately 3 nm. The coating thickness was estimated according to the particle size distribution difference between coated and uncoated particles, as measured by a TSI scanning mobility particle sizer. The coated particles were subsequently sent into the OFR (15 μg m^{-3}; measured with an Aerodyne high-resolution time-of-flight aerosol mass spectrometer (HR-TOF-AMS)).[19] In the OFR, LCM particles were exposed to OH radicals at 298 K which were formed via UV photolysis (254 nm) of ozone (0−2 ppm) with water vapor (35% RH). The OH exposure was in the range of 4.7×10^{10}−1.6×10^{12} molecules cm^{-3} s, as estimated via the decay of CO gas[20] inside the OFR during offline calibrations (see SI).

Product Analysis. Generally, the HR-TOF-AMS is not amenable to product identification due to the significant molecular fragmentation associated with the 70 eV electron impact ionization. Therefore, particle-phase heterogeneously derived oxidation products of LCMs were qualitatively identified with an EESI-TOFMS (electrospray ionization time-of-flight mass spectrometer) which provided online molecular information for organic particles,[21,22] as described further in the SI. The oxidized LCM particles first passed through a multichannel extruded carbon denuder to remove gas-phase organic compounds, followed by collision with electrospray droplets generated by an electrospray capillary, where soluble components were extracted. The evaporation of the droplets produced ions through the Coulomb explosion mechanism, which were subsequently analyzed by a Tofwerk atmospheric pressure interface time-of-flight mass spectrometer (APi-TOFMS). The electrospray working fluid was a CH_3CN−H_2O mixture (80:20 by volume) with 200 ppm of NaI as a charge carrier. Oxidation products were detected as adducts with Na^+ (i.e., in positive ion mode). For mass calibration, ions associated with $[(NaI)_x(H_2O)_y(CH_3CN)_z]$-$Na^+$ clusters, which were well spaced across the entire m/z range of interest (m/z 23−491) were used.[23]

RESULTS AND DISCUSSION

Reaction Kinetics. The effective heterogeneous reaction rate constants k_{eff} (cm^3 molecule^{-1} s^{-1}) were calculated by measuring the decay of particle-phase LCMs, as estimated using selected molecular marker ions from the HR-TOF-AMS that were proportional to LCM concentrations (m/z 306 for EPPB and m/z 318 for EFPT; see SI). The k_{eff} for the heterogeneous OH reaction with a LCM was calculated according to eq 1[15,24]

$$\ln\frac{I}{I_0} = -k_{eff}[OH]_{exp} \quad (1)$$

where I_0 and I are the initial and current LCM concentrations in the presence of OH radicals, respectively, and $[OH]_{exp}$ represents the OH exposure. The k_{eff} can be determined from the plot of I/I_0 as a function of $[OH]_{exp}$ (Figure S1), after fitting an exponential function to the data. The effect of OH gas-phase diffusion on the measured k_{eff} was accounted for,[25,26] resulting in a calculated true rate constant (k).

https://dx.doi.org/10.1021/acs.estlett.0c00447
Environ. Sci. Technol. Lett. 2020, 7, 646−652

As shown in Table 1, the calculated values of k for EPPB and EFPT are $(7.05 \pm 0.46) \times 10^{-13}$ and $(4.67 \pm 0.25) \times 10^{-13}$ cm^3 $molecule^{-1}$ s^{-1}, respectively. These values of k are less than those of phosphate flame retardants such as tris-1,3-dichloro-2-propyl phosphate (9.20×10^{-13} cm^3 $molecule^{-1}$ s^{-1}) and 2-ethylhexyl diphenyl phosphate (1.12×10^{-12} cm^3 $molecule^{-1}$ s^{-1}),[15,23] suggesting a lower OH reactivity of EPPB and EFPT relative to phosphate flame retardants. As noted above, a previous study has based the determination of the atmospheric persistence of LCMs on AOPWIN-modeled rate constants,[3] which are also provided in Table 1 for EPPB and EFPT. The derived kinetic data here for these two compounds indicate that the measured k values are 30 times lower than the modeled results. The significant differences between the measured and modeled rate constants for these two LCMs reflect the ineffectiveness of currently used models to predict the reactivity for particulate compounds and has important implications for the atmospheric fate of currently produced LCMs, as discussed further below.

Oxidation Products and Mechanisms. In addition to the heterogeneous kinetics derived above, an important aspect associated with the fate of LCMs is an understanding of the oxidation products upon photooxidation. Such information can be determined through the use of an EESI-TOFMS (see Materials and Methods). The difference in the EESI-TOFMS spectra between oxidized and unreacted LCM-containing particles is illustrated in Figure 1A and B for EPPB and EFPT, respectively.

In the case of EPPB, the signal intensities for m/z peaks at 329 and 370, which were attributed to $[M+Na^+]$, and $[M(CH_3CN)]Na^+$ (M = EPPB molecule), decreased substantially when exposed to OH radicals (Figure 1A), consistent with the degradation of EPPB. Conversely, a number of m/z peaks (m/z 269−436) increased because of the presence of transformation products (possible structures shown in Table S2) which clustered with Na^+ ions. On the basis of the tentatively identified particulate products from the EPPB oxidation experiments, a general photooxidation mechanism for particulate EPPB was proposed, where black boxes indicated chemical formulas that were identified by EESI-TOFMS during experiments (Figure 2A). The oxidation reactions in Figure 2A include two major channels: OH reactions with the alkyl group (channel 1) and with the phenyl ring (channel 2).

In channel 1, oxidation is initiated by H-abstraction by OH from the propyl group of EPPB in the presence of O_2, generating alkylperoxy radicals. A hydroperoxide (product E_1) is formed during the subsequent reactions of alkylperoxy radicals and HO_2, which can further react via two additional oxidation routes. First, E_1 is converted to an alcohol (product E_2) and a carbonyl (product E_3) through the well-known Russell mechanism,[27,28] which are subsequently oxidized to an organic acid (product E_4) and a peracid (product E_5), respectively. Second, a dihydroperoxide (product E_6) and a trihydroperoxide (product E_{14}) were formed during the reactions of E_1 and OH, which can then be converted to hydroxyl hydroperoxides (products E_7 and E_{15}) and carbonyl hydroperoxides (products E_8 and E_{16}) via the above-mentioned Russell mechanism, respectively. With continued OH reaction, E_8 can be converted to carbonyls (products E_9 and E_{12}), a dicarbonyl hydroperoxide (product E_{10}), a hydroxyl dicarbonyl (product E_{11}), and a carboxyl hydroperoxide (product E_{13}).

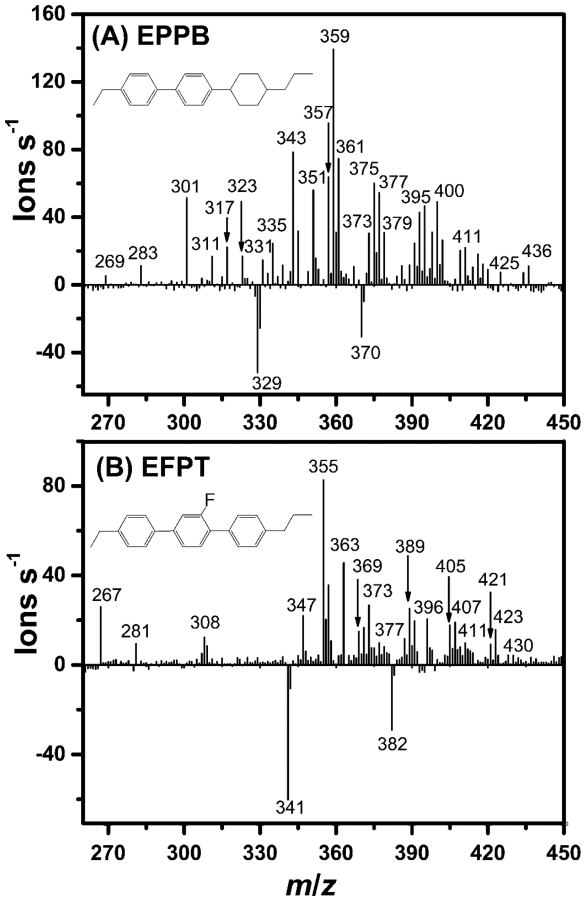

Figure 1. Differential EESI-TOFMS spectra (oxidized−unreacted) for EPPB (A) and EFPT (B) at 6.1×10^{11} and 1.1×10^{12} molecules cm^{-3} s OH exposure, respectively. Positive mass spectra indicate formed products. For clarity, the $[(NaI)_x(H_2O)_y(CH_3CN)_z]Na^+$ ions were removed.

Channel 2 proceeds via a well-established OH-addition mechanism,[29,30] whereby a phenol product (product E_{17}) can be formed directly, as well as O_2 addition to produce cyclic peroxy radicals (see the blue box in Figure 2A). The cyclic peroxy radicals are in turn converted to cyclic hydroxyl hydroperoxides (product E_{18}) or are isomerized to carbon-centered radicals (see the purple box in Figure 2A). With further O_2 addition, these carbon-centered radicals lead to the formation of bicyclic peroxy radicals, which have been demonstrated to be key photooxidation intermediates for aromatic compounds such as toluene and m-xylene.[31,32] Once formed, bicyclic peroxy radicals can undergo two reaction pathways. The first pathway involves a non-ring-opening reaction; i.e., bicyclic peroxy intermediates react with HO_2 to produce a bicyclic hydroxyl hydroperoxide (product E_{21}), which subsequently transforms to a bicyclic alcohol (product E_{22}) and a bicyclic carbonyl (product E_{23}). In the second pathway, bicyclic peroxy intermediates undergo ring-opening reactions to form unsaturated dicarbonyls (product E_{24} and E_{28}). Further reaction of E_{18}, E_{24}, and E_{28} would result in the formation of products E_{19}−E_{20} (cyclic alcohols and carbonyls), E_{25}−E_{27} (unsaturated carboxylic acids), and E_{29}−E_{32} (unsaturated hydroperoxides, alcohols, and carbonyls), respectively.

The mechanisms presented above are consistent with mechanisms for the photooxidation of alkanes[33,34] and

https://dx.doi.org/10.1021/acs.estlett.0c00447
Environ. Sci. Technol. Lett. 2020, 7, 646−652

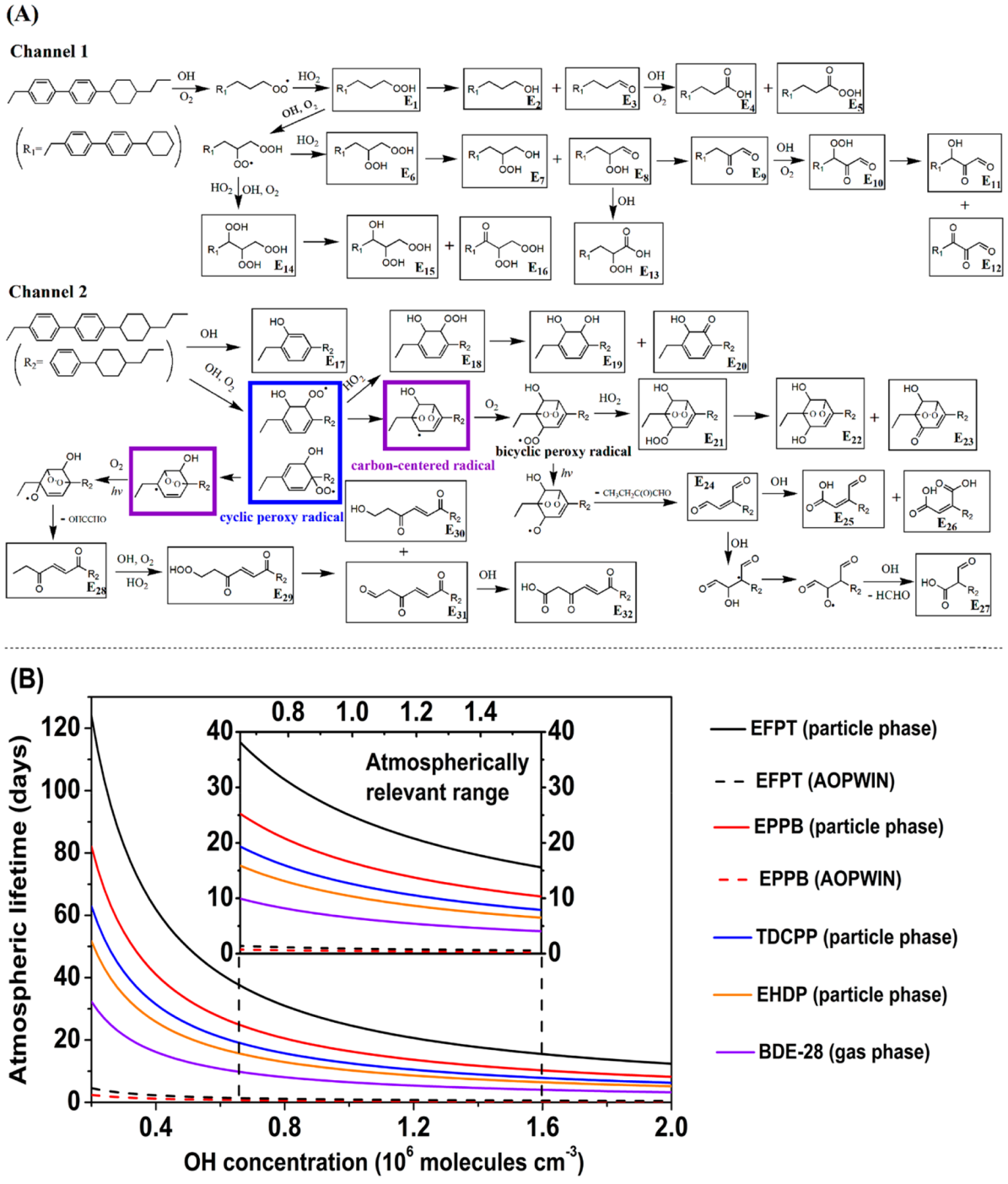

Figure 2. (A) Proposed heterogeneous photooxidation mechanism for particle-phase EPPB. The black boxes indicate oxidation products (i.e., elemental formulas) measured using the EESI-TOFMS. Note that the mechanism presented is not a complete mechanism for the heterogeneous OH oxidation of EPPB, as oxidation may also occur on the ethyl, phenyl, and cyclohexyl groups, potentially forming isomers not shown. (B) Estimated atmospheric lifetimes of EPPB, EFPT, and flame retardants (TDCPP, EHDP, and BDE-28).[15,23,41] BDE-28: 2,4,4′-tribrominated diphenyl ether. The atmospheric lifetimes for particle-phase species were estimated using measured heterogeneous kinetics data.

aromatic compounds,[31,35] respectively. In addition, some products of EPPB (e.g., E_{19}) can undergo further reactions to form products E_{33}−E_{40}, as shown in Figure S2. Together, 40 oxidation products are observed for EPPB, among which E_1 and E_{20} (m/z 361), E_2 and E_{17} (m/z 345), E_5 and E_8 (m/z 375), and E_6 and E_{23} (m/z 393) are isomers (with identical exact mass), and cannot be differentiated from each other.

With respect to EFPT, the signal intensities at m/z ions 341 and 382, which were ascribed to $[M+Na^+]$ and $[M(CH_3CN)]$-Na^+ (M = EFPT molecule), decreased significantly when exposed to OH radicals (Figure 1B). At the same time, multiple m/z ions in the range of from m/z 267 to 430 increased, having ions associated with Na^+ or $(CH_3CN)Na^+$ clusters with oxidation products F_1−F_{26}, as shown in Table S3. Upon the basis of the tentatively identified products in Table S3, we propose a photooxidation mechanism for EFPT (Figure S3) which is similar to that of EPPB (i.e., channel 1 and channel 2 in Figure 2A). The similarity between mechanisms

https://dx.doi.org/10.1021/acs.estlett.0c00447
Environ. Sci. Technol. Lett. 2020, 7, 646−652

here implies that other particulate LCMs may follow similar reaction mechanisms during photooxidation. This is particularly likely since currently produced LCMs have similar chemical structures,[3] i.e., diphenyl backbone structure with possible halogen substitution. Consequently, the photooxidation products for particulate LCMs may potentially be predicted based upon the currently proposed mechanisms, with important implications described below.

It should be noted that the reaction channels presented here (Figure 2A and Figure S3) represent a general photooxidation mechanism for particulate LCMs, since oxidation can also occur on other reactive sites including the ethyl, phenyl, and cyclohexyl groups (probability discussed in SI), with the potential for the formation of additional isomers. Regardless, the evolution of the identified oxidation products during photooxidation is consistent with the currently proposed oxidation mechanisms, in that the relative signal enhancements for early generation products with increased OH exposure are generally more prominent than those of later-generation products (Figure S4). The HR-TOF-AMS results can also offer some limited insights into the LCMs transformation products, which are in agreement with the EESI-TOFMS results (see SI).

Atmospheric Persistence and Implications. With the measured kinetic rate constants provided here (Table 1), a more accurate picture of the atmospheric persistence of these LCM emerges. The atmospheric lifetimes τ (days), which are important parameters for determining the risks of synthetic chemicals,[36,37] can be estimated for EPPB and EFPT based upon a global mean OH concentration ($[OH]_{GM}$; 6.5×10^5–1.6×10^6 molecules cm^{-3})[38−40] and the reaction rate constants determined here (k)

$$\tau = 1/k[OH]_{GM} \quad (2)$$

The calculated τ_{EPPB} and τ_{EFPT} are in the ranges of 10.3−25.3 and 15.5−38.1 days, respectively. The lifetimes determined here, while dependent on the concentration of $[OH]_{GM}$, are ∼30 times longer than those estimated previously through modeling (Figure 2B). Previous results have also demonstrated that other synthetic chemicals (e.g., flame retardants) are more persistent than predicted, similarly as a result of large deviations between measured heterogeneous kinetics and AOPWIN modeled gas-phase kinetics.[15,16]

We note that the atmospheric lifetimes derived for EPPB (up to 25 days) and EFPT (up to 38 days) are significantly longer than the τ of flame retardants such as tris-1,3-dichloro-2-propyl phosphate, 2-ethylhexyl diphenyl phosphate, and 2,4,4′-tribromodiphenyl ether (up to 10−19 days; Figure 2B),[15,23,41] all of which have been demonstrated to be persistent in air and can undergo long-range transport.[42,43] Therefore, the two investigated LCMs, and likely other low volatility LCMs of similar structure (∼190 LCMs; see SI), will also be persistent in the atmosphere, with the potential to undergo long-range atmospheric transport. This is contrary to previous understanding, which until now has considered LCMs to be nonpersistent in air.[3] Consequently, LCMs may be ubiquitous in the outdoor environment, despite no published reports of their measurements in ambient air. With the demonstrated health impacts associated with LCMs,[3] the present results highlight the need for future ambient field measurement studies, potentially utilizing passive air sampling for long-term monitoring,[44,45] to quantify the levels of LCMs in various regions globally, as a first step in assessing the environmental and health risks of these chemicals. Similarly, this work indicates that LCMs are also likely to be persistent within indoor environments, which are known to contain oxidants[46,47] and numerous LCD device sources.

The present study, while offering new kinetic results for LCMs, also provides valuable insights into the oxidation mechanisms and products for airborne particulate LCM. The product information here is likely to provide guidance for future field measurements that aim to understand the fate of LCMs, including their oxidation products in both indoor and outdoor environments. This represents the logical next step in further understanding the overall impacts of LCM oxidative chemistry.

Furthermore, the recent proliferation of nontargeted analysis as a means of identifying pollutants in environmental samples[48−50] provides additional support for the current work. The interpretation and source characterization of the resultant complex nontargeted data sets are extremely difficult due to the lack of information on the chemical characteristics of the detected compounds (parent molecule vs transformation product).[51] However, based upon the product information obtained here, the nontargeted analysis process can be simplified via a suspect screening approach, whereby field sample data are scrutinized for the presence of LCM products determined here. This will significantly enhance the data processing efficiency of nontargeted analysis, particularly since the current results suggest that the heterogeneous oxidation products from other LCMs of similar structure can be predicted.

It should also be noted that quantification of the oxidation products in this work cannot currently be achieved due to the lack of product standards. Despite this limitation, the complexity of LCM products observed here (66 species, not including isomers) for just two parent compounds underscores the need for additional investigations into these chemicals. This must include further study of the toxicity of the parent LCM as well as the toxicological evolution of LCMs upon photooxidation, as it remains an open question whether the overall LCM matrix (parent + products) will become more or less toxic upon introduction to the atmosphere. This will contribute to a more complete understanding of the environmental and health risks associated with atmospheric LCMs.

■ ASSOCIATED CONTENT

Supporting Information

The Supporting Information is available free of charge at https://pubs.acs.org/doi/10.1021/acs.estlett.0c00447.

OFR experiments, EESI-TOFMS measurements, HR-TOF-AMS results, other aspects of photooxidation mechanism, and the number of LCMs with long-range atmospheric transport potential. LCM kinetics (Figure S1), formation of products E_{33}−E_{40} during photooxidation of EPPB (Figure S2), photooxidation mechanism of EFPT (Figure S3), EESI-TOFMS signal intensities for oxidation products at different OH exposures (Figure S4), HR-TOF-AMS spectra (Figure S5), LCM fragments measured by HR-TOF-AMS (Figure S6), physiochemical properties of LCMs (Table S1), identified products for EPPB (Table S2), and identified products for EFPT (Table S3). (PDF)

https://dx.doi.org/10.1021/acs.estlett.0c00447
Environ. Sci. Technol. Lett. 2020, 7, 646−652

AUTHOR INFORMATION

Corresponding Author

John Liggio − *Air Quality Processes Research Section, Environment and Climate Change Canada, Toronto, Ontario M3H 5T4, Canada;* orcid.org/0000-0003-3683-4595; Phone: 1-416-739-4840; Email: John.Liggio@canada.ca

Authors

Qifan Liu − *Air Quality Processes Research Section, Environment and Climate Change Canada, Toronto, Ontario M3H 5T4, Canada;* orcid.org/0000-0003-0033-5313

Jeremy Wentzell − *Air Quality Processes Research Section, Environment and Climate Change Canada, Toronto, Ontario M3H 5T4, Canada*

Patrick Lee − *Air Quality Processes Research Section, Environment and Climate Change Canada, Toronto, Ontario M3H 5T4, Canada*

Kun Li − *Air Quality Processes Research Section, Environment and Climate Change Canada, Toronto, Ontario M3H 5T4, Canada;* orcid.org/0000-0003-2970-037X

Shao-Meng Li − *Air Quality Processes Research Section, Environment and Climate Change Canada, Toronto, Ontario M3H 5T4, Canada;* orcid.org/0000-0002-7628-6581

Complete contact information is available at: https://pubs.acs.org/10.1021/acs.estlett.0c00447

Notes

The authors declare no competing financial interest.

ACKNOWLEDGMENTS

We would like to thank Dr. Tom Harner for helpful discussions. This work was partially funded by the air pollution program and the chemicals management plan program of Environment and Climate Change Canada.

REFERENCES

(1) Li, J.; Su, G.; Letcher, R. J.; Xu, W.; Yang, M.; Zhang, Y. Liquid crystal monomers (LCMs): a new generation of persistent bioaccumulative and toxic (PBT) compounds? *Environ. Sci. Technol.* **2018**, *52*, 5005−5006.

(2) Schultz, J.; Chartoff, R. Photopolymerization of nematic liquid crystal monomers for structural applications: molecular order and orientation dynamics. *Polymer* **1998**, *39*, 319−325.

(3) Su, H.; Shi, S.; Zhu, M.; Crump, D.; Letcher, R. J.; Giesy, J. P.; Su, G. Persistent, bioaccumulative, and toxic properties of liquid crystal monomers and their detection in indoor residential dust. *Proc. Natl. Acad. Sci. U. S. A.* **2019**, *116*, 26450−26458.

(4) Orbis Research. *Global liquid crystal monomer market analysis 2013−2018 and forecast 2019−2024.* https://www.orbisresearch.com/reports/index/global-liquid-crystal-monomer-market-analysis-2013-2018-and-forecast-2019-2024 (accessed 5 April 2019).

(5) IHS Markit. https://ihsmarkit.com/index.html (accessed 20 March 2019).

(6) Woolverton, C. J.; Gustely, E.; Li, L.; Lavrentovich, O. D. Liquid crystal effects on bacterial viability. *Liq. Cryst.* **2005**, *32*, 417−423.

(7) Gligorovski, S.; Strekowski, R.; Barbati, S.; Vione, D. Environmental implications of hydroxyl radicals ($^{\bullet}$OH). *Chem. Rev.* **2015**, *115*, 13051−13092.

(8) Aschmann, S. M.; Tuazon, E. C.; Atkinson, R. Atmospheric chemistry of diethyl methylphosphonate, diethyl ethylphosphonate, and triethyl phosphate. *J. Phys. Chem. A* **2005**, *109*, 2282−2291.

(9) Laversin, H.; El Masri, A.; Al Rashidi, M.; Roth, E.; Chakir, A. Kinetic of the gas-phase reactions of OH radicals and Cl atoms with diethyl ethylphosphonate and triethyl phosphate. *Atmos. Environ.* **2016**, *126*, 250−257.

(10) Murschell, T.; Farmer, D. K. Atmospheric OH oxidation of three chlorinated aromatic herbicides. *Environ. Sci. Technol.* **2018**, *52*, 4583−4591.

(11) Moriarty, J.; Sidebottom, H.; Wenger, J.; Mellouki, A.; Le Bras, G. Kinetic studies on the reactions of hydroxyl radicals with cyclic ethers and aliphatic diethers. *J. Phys. Chem. A* **2003**, *107*, 1499−1505.

(12) Coeur-Tourneur, C.; Cassez, A.; Wenger, J. C. Rate coefficients for the gas-phase reaction of hydroxyl radicals with 2-methoxyphenol (guaiacol) and related compounds. *J. Phys. Chem. A* **2010**, *114*, 11645−11650.

(13) Lauraguais, A.; Bejan, I.; Barnes, I.; Wiesen, P.; Coeur, C. Rate coefficients for the gas-phase reactions of hydroxyl radicals with a series of methoxylated aromatic compounds. *J. Phys. Chem. A* **2015**, *119*, 6179−6187.

(14) Alton, M.; Browne, E. C. Atmospheric chemistry of volatile methyl siloxanes: kinetics and products of oxidation by OH radicals and Cl atoms. *Environ. Sci. Technol.* **2020**, *54*, 5992−5999.

(15) Liu, Y.; Liggio, J.; Harner, T.; Jantunen, L.; Shoeib, M.; Li, S. M. Heterogeneous OH initiated oxidation: a possible explanation for the persistence of organophosphate flame retardants in air. *Environ. Sci. Technol.* **2014**, *48*, 1041−1048.

(16) Liu, Q.; Liggio, J.; Li, K.; Lee, P.; Li, S. M. Understanding the impact of relative humidity and coexisting soluble iron on the OH-initiated heterogeneous oxidation of organophosphate flame retardants. *Environ. Sci. Technol.* **2019**, *53*, 6794−6803.

(17) Lai, C.; Liu, Y.; Ma, J.; Ma, Q.; He, H. Degradation kinetics of levoglucosan initiated by hydroxyl radical under different environmental conditions. *Atmos. Environ.* **2014**, *91*, 32−39.

(18) Liu, C.; He, Y.; Chen, X. Kinetic study on the heterogeneous degradation of coniferyl alcohol by OH radicals. *Chemosphere* **2020**, *241*, 125088.

(19) DeCarlo, P. F.; Kimmel, J. R.; Trimborn, A.; Northway, M. J.; Jayne, J. T.; Aiken, A. C.; Gonin, M.; Fuhrer, K.; Horvath, T.; Docherty, K. S.; et al. Field-deployable, high-resolution, time-of-flight aerosol mass spectrometer. *Anal. Chem.* **2006**, *78*, 8281−8289.

(20) Liu, Y.; Sander, S. P. Rate constant for the OH + CO reaction at low temperatures. *J. Phys. Chem. A* **2015**, *119*, 10060−10066.

(21) Lopez-Hilfiker, F. D.; Pospisilova, V.; Huang, W.; Kalberer, M.; Mohr, C.; Stefenelli, G.; Thornton, J. A.; Baltensperger, U.; Prevot, A. S.; Slowik, J. G. An extractive electrospray ionization time-of-flight mass spectrometer (EESI-TOF) for online measurement of atmospheric aerosol particles. *Atmos. Meas. Tech.* **2019**, *12*, 4867−4886.

(22) Qi, L.; Chen, M.; Stefenelli, G.; Pospisilova, V.; Tong, Y.; Bertrand, A.; Hueglin, C.; Ge, X.; Baltensperger, U.; Prévôt, A. S. H.; et al. Organic aerosol source apportionment in Zurich using an extractive electrospray ionization time-of-flight mass spectrometer (EESI-TOF-MS)-Part 2: biomass burning influences in winter. *Atmos. Chem. Phys.* **2019**, *19*, 8037−8062.

(23) Liu, Q.; Liggio, J.; Wu, D.; Saini, A.; Halappanavar, S.; Wentzell, J. J.; Harner, T.; Li, K.; Lee, P.; Li, S. M. Experimental study of OH-initiated heterogeneous oxidation of organophosphate flame retardants: kinetics, mechanism, and toxicity. *Environ. Sci. Technol.* **2019**, *53*, 14398−14408.

(24) Chan, M. N.; Zhang, H.; Goldstein, A. H.; Wilson, K. R. Role of water and phase in the heterogeneous oxidation of solid and aqueous succinic acid aerosol by hydroxyl radicals. *J. Phys. Chem. C* **2014**, *118*, 28978−28992.

(25) Worsnop, D.; Morris, J.; Shi, Q.; Davidovits, P.; Kolb, C. A chemical kinetic model for reactive transformations of aerosol particles. *Geophys. Res. Lett.* **2002**, *29*, 57-1−57-4.

(26) Fuks, N. A.; Sutugin, A. G. *Highly Dispersed Aerosols*; Butterworth-Heinemann: Newton, MA, 1970.

(27) Miyamoto, S.; Martinez, G. R.; Medeiros, M. H.; Di Mascio, P. Singlet molecular oxygen generated from lipid hydroperoxides by the Russell mechanism: studies using ^{18}O-labeled linoleic acid hydroperoxide and monomol light emission measurements. *J. Am. Chem. Soc.* **2003**, *125*, 6172−6179.

(28) Russell, G. A. Deuterium-isotope effects in the autoxidation of aralkyl hydrocarbons. mechanism of the interaction of peroxy radicals1. *J. Am. Chem. Soc.* **1957**, *79*, 3871−3877.
(29) Wu, R.; Pan, S.; Li, Y.; Wang, L. Atmospheric oxidation mechanism of toluene. *J. Phys. Chem. A* **2014**, *118*, 4533−4547.
(30) Baltaretu, C. O.; Lichtman, E. I.; Hadler, A. B.; Elrod, M. J. Primary atmospheric oxidation mechanism for toluene. *J. Phys. Chem. A* **2009**, *113*, 221−230.
(31) Birdsall, A. W.; Andreoni, J. F.; Elrod, M. J. Investigation of the role of bicyclic peroxy radicals in the oxidation mechanism of toluene. *J. Phys. Chem. A* **2010**, *114*, 10655−10663.
(32) Zhang, Q.; Xu, Y.; Jia, L. Secondary organic aerosol formation from OH-initiated oxidation of *m*-xylene: effects of relative humidity on yield and chemical composition. *Atmos. Chem. Phys.* **2019**, *19*, 15007−15021.
(33) Yee, L.; Craven, J.; Loza, C.; Schilling, K.; Ng, N.; Canagaratna, M.; Ziemann, P.; Flagan, R.; Seinfeld, J. Effect of chemical structure on secondary organic aerosol formation from C12 alkanes. *Atmos. Chem. Phys.* **2013**, *13*, 11121−11140.
(34) Schilling Fahnestock, K. A.; Yee, L. D.; Loza, C. L.; Coggon, M. M.; Schwantes, R.; Zhang, X.; Dalleska, N. F.; Seinfeld, J. H. Secondary organic aerosol composition from C12 alkanes. *J. Phys. Chem. A* **2015**, *119*, 4281−4297.
(35) Yang, Z.; Tsona, N. T.; Li, J.; Wang, S.; Xu, L.; You, B.; Du, L. Effects of NO_x and SO_2 on the secondary organic aerosol formation from the photooxidation of 1, 3, 5-trimethylbenzene: a new source of organosulfates. *Environ. Pollut.* **2020**, *264*, 114742.
(36) Liagkouridis, I.; Cousins, A. P.; Cousins, I. T. Physical−chemical properties and evaluative fate modelling of 'emerging' and 'novel' brominated and organophosphorus flame retardants in the indoor and outdoor environment. *Sci. Total Environ.* **2015**, *524*, 416−426.
(37) Cousins, I. T.; Ng, C. A.; Wang, Z.; Scheringer, M. Why is high persistence alone a major cause of concern? *Environ. Sci.: Processes Impacts* **2019**, *21*, 781−792.
(38) Prinn, R.; Huang, J.; Weiss, R.; Cunnold, D.; Fraser, P.; Simmonds, P.; McCulloch, A.; Harth, C.; Salameh, P.; O'doherty, S.; et al. Evidence for substantial variations of atmospheric hydroxyl radicals in the past two decades. *Science* **2001**, *292*, 1882−1888.
(39) Lawrence, M. G.; Jockel, P.; von Kuhlmann, R. What does the global mean OH concentration tell us? *Atmos. Chem. Phys.* **2001**, *1*, 37−49.
(40) Mao, J.; Ren, X.; Brune, W.; Olson, J.; Crawford, J.; Fried, A.; Huey, L.; Cohen, R.; Heikes, B.; Singh, H.; et al. Airborne measurement of OH reactivity during INTEX-B. *Atmos. Chem. Phys.* **2009**, *9*, 163−173.
(41) Cao, H.; He, M.; Han, D.; Li, J.; Li, M.; Wang, W.; Yao, S. OH-initiated oxidation mechanisms and kinetics of 2, 4, 4′-tribrominated diphenyl ether. *Environ. Sci. Technol.* **2013**, *47*, 8238−8247.
(42) Möller, A.; Sturm, R.; Xie, Z.; Cai, M.; He, J.; Ebinghaus, R. Organophosphorus flame retardants and plasticizers in airborne particles over the Northern Pacific and Indian Ocean toward the polar regions: evidence for global occurrence. *Environ. Sci. Technol.* **2012**, *46*, 3127−3134.
(43) Mulder, M. D.; Heil, A.; Kukučka, P.; Kuta, J.; Přibylová, P.; Prokeš, R.; Lammel, G. Long-range atmospheric transport of PAHs, PCBs and PBDEs to the central and eastern Mediterranean and changes of PCB and PBDE congener patterns in summer 2010. *Atmos. Environ.* **2015**, *111*, 51−59.
(44) Saini, A.; Clarke, J.; Jariyasopit, N.; Rauert, C.; Schuster, J. K.; Halappanavar, S.; Evans, G. J.; Su, Y.; Harner, T. Flame retardants in urban air: a case study in Toronto targeting distinct source sectors. *Environ. Pollut.* **2019**, *247*, 89−97.
(45) Schuster, J. K.; Harner, T.; Su, K.; Eng, A.; Wnorowski, A.; Charland, J. P. Temporal and spatial trends of polycyclic aromatic compounds in air across the Athabasca oil sands region reflect inputs from open pit mining and forest fires. *Environ. Sci. Technol. Lett.* **2019**, *6*, 178−183.
(46) Young, C. J.; Zhou, S.; Siegel, J. A.; Kahan, T. F. Illuminating the dark side of indoor oxidants. *Environ. Sci.: Processes Impacts* **2019**, *21*, 1229−1239.
(47) Abbatt, J. P.; Wang, C. The atmospheric chemistry of indoor environments. *Environ. Sci.: Processes Impacts* **2020**, *22*, 25−48.
(48) Hollender, J.; Schymanski, E. L.; Singer, H. P.; Ferguson, P. L. Nontarget screening with high resolution mass spectrometry in the environment: ready to go? *Environ. Sci. Technol.* **2017**, *51*, 11505−11512.
(49) Sun, C.; Zhang, Y.; Alessi, D. S.; Martin, J. W. Nontarget profiling of organic compounds in a temporal series of hydraulic fracturing flowback and produced waters. *Environ. Int.* **2019**, *131*, 104944.
(50) Giorio, C.; Bortolini, C.; Kourtchev, I.; Tapparo, A.; Bogialli, S.; Kalberer, M. Direct target and non-target analysis of urban aerosol sample extracts using atmospheric pressure photoionisation high-resolution mass spectrometry. *Chemosphere* **2019**, *224*, 786−795.
(51) Schymanski, E. L.; Singer, H. P.; Slobodnik, J.; Ipolyi, I. M.; Oswald, P.; Krauss, M.; Schulze, T.; Haglund, P.; Letzel, T.; Grosse, S.; et al. Non-target screening with high-resolution mass spectrometry: critical review using a collaborative trial on water analysis. *Anal. Bioanal. Chem.* **2015**, *407*, 6237−6255.

https://dx.doi.org/10.1021/acs.estlett.0c00447
Environ. Sci. Technol. Lett. 2020, 7, 646−652